Toward Total Implantability Using Free-Range Resonant Electrical Energy Delivery System: Achieving Untethered Ventricular Assist Device Operation Over Large Distances

Benjamin Waters, BS[a], Alanson Sample, PhD[a], Joshua Smith, PhD[a,b], Pramod Bonde, MD[c,*]

KEYWORDS

• Free-Range Resonant Electrical Energy Delivery system
• Ventricular assist device • Heart disease • Heart failure
• Wireless power • Mechanical support

THE PROBLEM

Heart failure is a terminal disease with a very poor prognosis and constitutes Medicare's greatest area of spending, with annual expenditures close to $35 billion.[1] The gold standard of treatment for this disease remains heart transplant; however, only a minority (approximately 2000 per year) of patients can benefit from transplants because of continuing donor shortage.

Another alternative, which has shown promise, is mechanical circulatory assistance with ventricular assist devices (VAD).[1] An estimated 100,000 patients worldwide can benefit from VAD therapy.[1] The benefit of VAD technology was demonstrated by the randomized evaluation of mechanical assistance for the treatment of congestive heart failure trial, which showed a 50% survival benefit for patients assigned to the VAD arm compared with those undergoing maximal medical management.[2] The same trial, however, also showed the limitations with the first-generation VADs in terms of large size and mechanical failure.[2–4] These findings prompted researchers and industry to concentrate their efforts in minimizing the size of the device, which has been achieved in the past decade with miniature axial and centrifugal pump technology. This advancement has allowed the use of these devices in smaller patients, who were not candidates in the past.[5]

[a] Department of Electrical Engineering, University of Washington, Box 352350,185 Stevens Way, Seattle, WA 98195-2350, USA
[b] Department of Computer Science and Engineering, University of Washington, Box 352350,185 Stevens Way, Seattle, WA 98195-2350, USA
[c] Section of Cardiac Surgery, Yale School of Medicine, 330 Cedar Street, Boardman 204, New Haven, CT 06520, USA
* Corresponding author.
E-mail address: prambond@hotmail.com

Cardiol Clin 29 (2011) 609–625
doi:10.1016/j.ccl.2011.08.002

Table 1
Distribution of ESIs among various risk categories

Variable	Non-ESI %	ESI %	*P* Value
Before 2000	55	45	*P*<.001
After 2000	80	20	
Nonobese	78	22	*P*<.03
Obese	65	35	
Cannula	69	31	*P* = .03
Driveline	78	22	
LVAD	77	23	*P* = .09
BiVAD	67	33	
Continuous	82	18	*P* = .17
Pulsatile	75	25	
Elective	81	19	*P* = .42
Nonelective	72	28	

Abbreviations: BiVAD, biventricular assist device; LVAD, left ventricular assist device.

A highly conservative approach is still practiced when offering VAD therapy to end-stage heart failure patients because of the associated adverse events, predominantly including the occurrence of repeated infections.[6] Infections occur despite the improved technology that typifies the smaller, durable designs with a single moving part that were introduced in the past decade.

Full advantage of these improvements is not realized because of essentially unchanged peripherals, including the percutaneous driveline for data retrieval and power supply.

A relationship among exit site infections (ESIs), pump pocket infection, and subsequent sepsis has been clearly shown. ESIs are influenced by constant exposure to the outside environment. Patients receiving VADs experience repeated infections, necessitating multiple antibiotics and repeated hospitalizations for surgical debridements. Infection also poses a therapeutic dilemma in terms of ever-increasing resistant colonization. ESIs often lead to subsequent pump infections, causing episodic bacteremia.[7–11]

Compared with other metallic implants (eg, cardiovascular implants, <2%; prosthetic valve endocarditis, 2%–4%[12,13]; orthopedic implants, such as hip and knee arthroplasty, <1%[14]), VADs pose a prohibitively high rate of infection, with reported incidence reaching 70% at the end of 1 year.[1–11,15–18]

VADs differ uniquely from other metallic implants because of the presence of a percutaneous drive line communicating with the exterior environment. As advancements move toward even longer durations of support on VADs,[4,5] the risk of ESIs continues to increase temporally, hampering quality of life and leading to repeated hospitalizations for antibiotic treatment or surgical interventions.[8,11,19–27] And, in rare instances, necessitating a pump exchange.[11,19] The net result of these infectious problems is reduced survival and increased cost, negating the intended benefits of VAD therapy.

Bonde and colleagues[28] examined 286 patients undergoing VAD implants at University of Pittsburgh Medical Center to focus on the incidence and temporal distribution of ESIs (**Table 1**). Actuarial freedom from ESIs at 6 months and 1 year was 60% and 45%, respectively. Between 0 and 3 months, 9.22 ESIs occurred per 100 patient months; at 3 to 6 months, 8.18 ESIs occurred per 100 patient months; and at 6 to 12 months the incidence decreased to 5.38 ESIs per 100 patient months (**Fig. 1**).

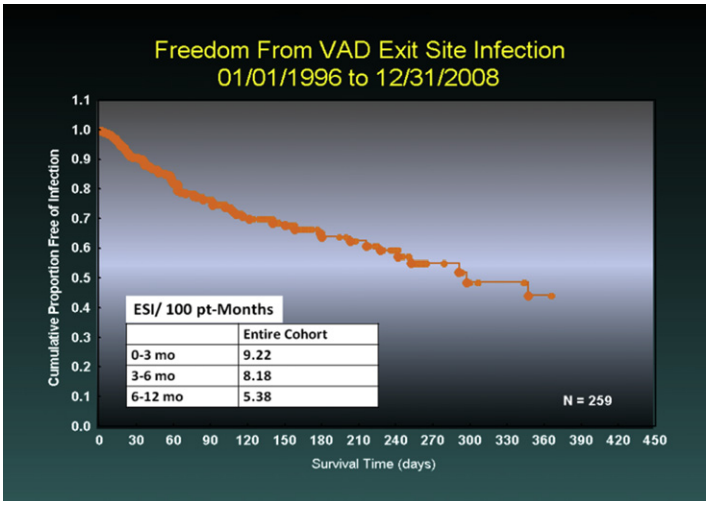

Fig. 1. Freedom from ESI in the entire cohort.

Time to first ESI was predominant in the first 90 days (Fig. 2). Recurrent ESIs were twice as common in pulsatile pumps than in continuous-flow VADs. Patients who developed early ESIs proceeded to develop late ESIs (n = 7, 100%).

National Trends in Readmissions After VAD Therapy

Bonde and colleagues[29] examined all adult patients undergoing a primary VAD implant from June 2006 to March 2010 from the prospective data entered in the interagency registry for mechanically assisted circulatory support registry. Patients were excluded who had subsequent right VAD implants or biventricular assist devices. The study examined 1586 patients (355 with a pulsatile pump and 1231 a rotary pump), and involved 192 deaths, 664 patients who were bridged to heart transplant, and 15 who experienced cardiac recovery. By 6 months 55% of patients were free of readmission, with stabilization between 1 and 3 years of 39% to 31% freedom from readmission. Freedom from readmission was not influenced by age, prior neurologic event, diabetes, intention to treat, diagnosis, or INTERMACS profile. Patients with rotary pumps showed significantly higher freedom from readmission beyond 1 year compared with those with pulsatile pumps (45% vs 27%, respectively; $P<.01$). Freedom from readmission was lower for those with ESIs ($P<.01$). The main known causes for first readmission remained ESIs (>70%). Patients who developed ESIs spent more time in the hospital and had 10 times as many readmissions compared with the cohort with no ESIs. Those with ESIs had reduced survival.

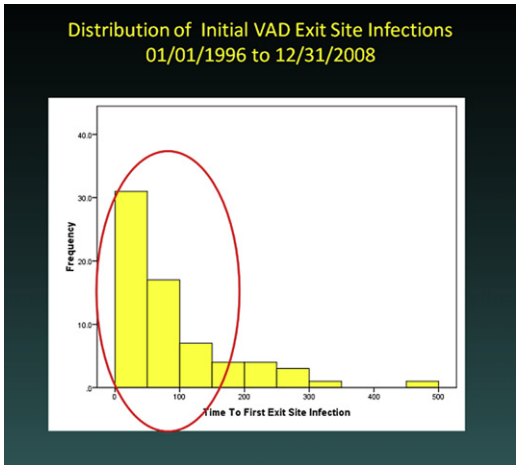

Fig. 2. Distribution of initial ESI.

THE SOLUTION

The solution to the problem is to power the VAD device remotely, thus eliminating the need for a percutaneous driveline. One of the primary aims of National Institutes of Health–funded research to support the development of VAD technology and artificial hearts has been to produce a totally implantable system capable of powering itself remotely with no drivelines traversing the skin. Industry and researchers addressed this using an induction-based transcutaneous energy transfer system (TETS).

Current Limitations of TETS

To address the problem of repeated driveline infections and reduced quality of life from permanently being tethered to a power console, industry and researchers attempted to develop a TETS using induction transfer.[6] However, after several decades of laboratory testing and prototype development, clinical application has been possible in only two systems ([Arrow LionHeart, Reading, PA, USA] and AbioCor TAH [ABIOMED, Inc, Danvers, MA, USA]). Clinical and laboratory experiences have shown several drawbacks with the current TETS technology, namely problems with alignment and the need for the transmitting and receiving coils to be located nearby.[6,7] The system incurs significant energy loss beyond 10 mm separation, resulting in significant heat generation.[7] The need for proximity means that the system must be implanted just under the skin and the external coil must be secured in position with adhesives; this poses various problems associated with skin irritability and thermal injury, which can result in burns. Any of these issues can result in a break in contact and catastrophic energy loss (this was one reason the Arrow LionHeart was withdrawn from the European market, a device which used TETS).[16] Continuous skin contact maintained with adhesives is not practical or clinically feasible, as was learned from transcutaneous drug delivery platforms that require users to change the site of application on a daily basis to prevent skin irritation and subsequent epithelial breakage. Although fraught with problems, the LionHeart trial showed overall reduced infections.

Innovation Through the Free-Range Resonant Electrical Energy Delivery System

Advances in wireless data communication have significantly improved the portability of electronic devices. More recently, wireless power technology offers the possibility of eliminating the remaining wired connection: the power cord. When used

with a VAD, wireless power technology will eliminate complications and infections caused by the percutaneous wired connection for implanted devices.

Several techniques exist to transmit power wirelessly from a transmitter to a receiver. For all methods, a tradeoff exists between the amount of power transferred and the separation distance between transmitter and receiver. Microwatts of power can be transferred over kilometer distances at high efficiencies using far-field techniques, whereas hundreds of watts can be transferred over meter distances at high efficiencies using near-field techniques. Some of the existing near-field applications, such as electronic toothbrushes and wireless charging pads, use inductive coupling techniques to charge devices over a few centimeters.

The Free-Range Resonant Electrical Energy Delivery (FREE-D) wireless power system uses magnetically coupled resonators to efficiently transfer power across meter distances to a VAD implanted in the human body. The transmit and receive resonators are essentially coils of wire that are tuned to resonate at a specific frequency. The resonator size and shape can be modified to accommodate application specifications, such as room size and patient body geometry. Additionally, an adaptive frequency tracking method can be implemented to achieve maximum power transfer efficiency, upwards of 70%, for nearly any angular orientation over a range of separation distances.

AIM

The authors propose to power a VAD device through strong resonant coupling technology, which affords seamless energy supply without compromising mobility or requiring direct contact between the individual and energy source.

SYSTEM OVERVIEW

Circuit Model

Fig. 3 shows a diagram of the basic magnetically coupled resonator wireless power system. The two-element transmitter consists of a single-turn drive resonator and a multiturn resonator that wirelessly transmits power to a two-element receiver that also consists of a single-turn drive resonator and multiturn resonator, but not necessarily with the same dimensions as the transmitter. These two resonant systems efficiently exchange energy

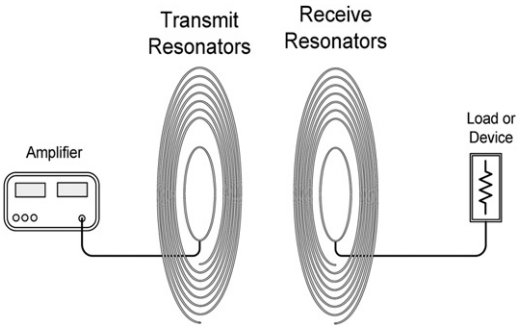

Fig. 3. Schematic of magnetically coupled resonators configuration.

through sharing nonradiative magnetic fields that oscillate at a specific frequency (approximately 7.65 MHz for this VAD application). The most significant interaction occurs between the two multiturn resonators, which are high-Q LCR tank resonators. These resonators share a mutual inductance that is a function of resonator geometry and separation distance between the resonators. When the receive resonator is within range of the magnetic field generated by the transmitter, power will be transferred wirelessly between the resonators.

Fig. 4 shows the circuit schematic for this system in terms of the lumped circuit elements L, C, and R. The transmit drive resonator and transmit multiturn resonator are modeled as inductors L_1 and L_2, and the receive drive resonator and multiturn resonator are modeled as inductors L_3 and L_4 respectively. Capacitors C_1 through C_4 are selected so that each magnetically coupled resonator will operate at the same resonant frequency according to the following equation:

$$f_{res} = \frac{1}{2\pi\sqrt{L_i C_i}}$$

The resistors R_1 through R_4 represent the parasitic resistances of the resonators, and are typically less than 1 Ω. Each resonant circuit is linked by the coupling coefficients k_{12}, k_{23}, and k_{34}. These coupling coefficients are typically an order of magnitude greater than the cross-coupling terms (k_{13}, k_{14}, and k_{24}), which have been neglected in the circuit analysis for simplicity. The transfer function shown below for the circuit model in **Fig. 2** is derived using Kirchhoff's voltage law:

$$\frac{V_L}{V_s} = \frac{j\omega^3 k_{12}k_{23}k_{34}L_2L_3\sqrt{L_1L_4R_L}}{k_{12}^2k_{34}^2L_1L_2L_3L_4\omega^4 + Z_1Z_2Z_3Z_4 + \omega^2\left(k_{12}^2L_1L_2Z_3Z_4 + k_{23}^2L_2L_3Z_1Z_4 + k_{34}^2L_3L_4Z_1Z_2\right)}$$

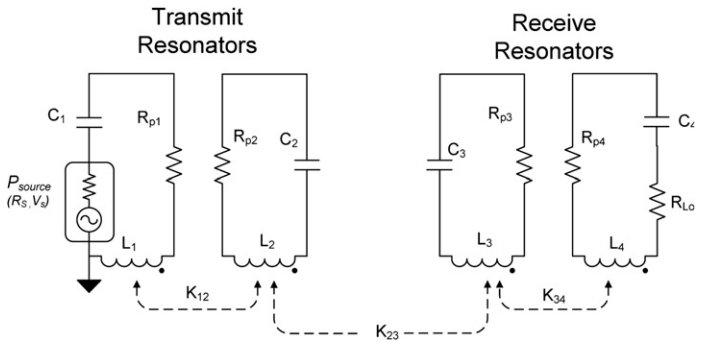

Fig. 4. Equivalent circuit model of the FREE-D system.

$$Z_1 = R_1 + R_3 + j\omega L_1 + \frac{1}{j\omega C_1}$$

$$Z_2 = R_2 + j\omega L_2 + \frac{1}{j\omega C_2}$$

$$Z_3 = R_3 + j\omega L_3 + \frac{1}{j\omega C_3}$$

$$Z_4 = R_4 + R_L + j\omega L_1 + \frac{1}{j\omega C_4}$$

Fig. 5 shows the *v*-shaped efficiency plateau for the large copper resonators used throughout the experiments discussed later. As the distance between the transmit and receive resonators increases, the amount of coupling between the resonators decreases, and the frequency separation also decreases until the two resonant peaks converge at f_{res}. In the overcoupled regime (distances <0.6 m in **Fig. 5**), the resonators share substantial magnetic flux and the system is capable of achieving maximum efficiency; in the undercoupled regime (distances >0.6 m in **Fig. 3**), the shared flux decreases below a threshold so that maximum efficiency cannot be achieved. Critical coupling is the point of transition between these two regimes, and corresponds to the greatest range at which maximum efficiency can be achieved. At any distance in the overcoupled regime, two different resonant frequencies are present in the magnetically coupled system, caused by the in-phase and out-of-phase modes of the overlapping magnetic fields. In this region, the efficiency can be maximized through tuning the frequency to the higher of these resonant peaks, as can be seen in the *v*-shaped curve in **Fig. 3**. In the undercoupled regime, wireless power transfer can still occur, but the maximum achievable efficiency is limited and declines rapidly with distance.

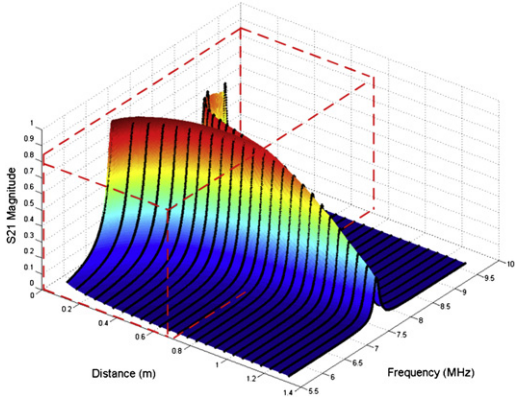

Fig. 5. Plot for FREE-D resonator efficiency (power gain) as a function of resonator separation distance and frequency.

FREE-D System for a VAD

One way to increase the range at which high power transfer efficiency can be achieved is to increase the size of the transmit and receive resonators. However, for use with a VAD, the size of the receive resonator is limited because it will be implanted in the human body. Therefore, another technique using a third relay resonator (**Fig. 6**) is implemented to accommodate greater separation distances between transmit and receive resonators. This relay resonator configuration is a practical design because several transmit resonators could be installed throughout a room (eg, walls, beds, couches, chairs), whereas a single relay resonator could be built into a jacket, much like the HeartMate GoGear Holster Vest (Thoratec Corporation, Pleasanton, California), worn by the patient, which would always be within range of the smaller receive resonator implanted in the patient's body. **Fig. 6** also shows a complete block diagram of the additional circuitry required to use the FREE-D system with a VAD. A radio

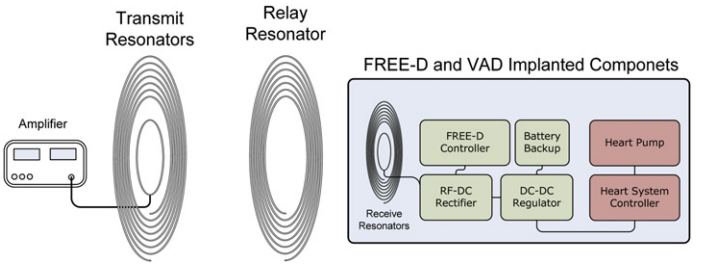

Fig. 6. Schematic of FREE-D for a VAD complete configuration.

frequency–direct current (RF-DC) rectifier is added to the receiver circuit to convert the oscillating RF signal to DC power. A DC-DC regulator steps down this DC voltage to a new DC voltage compatible with the VAD controller and VAD. A backup battery can provide power to the VAD controller intermittently in case FREE-D temporarily delivers insufficient power to the VAD controller. Ideally this battery will be rechargeable so that it can be charged by the FREE-D system with minimal access to the battery itself. This receiver circuitry and experimental configuration is shown in **Figs. 7** and **8**.

SAFETY OF FREE-D SYSTEM

Like all wireless devices, wireless power systems must respect two sets of regulations: electromagnetic interference (EMI) and safety. If the system uses an industrial, scientific, and medical (ISM) frequency band, such as 13.56 MHz, and does not encode data in the power carrier, then it is subject to Federal Communications Commission (FCC) part 18 regulations, and not to FCC part 15 regulations; operating in this fashion, the part 18 EMI regulations do not limit the transmitted power. (Part 18 does place limits on out-of-band emissions; this will require the use of high-quality waveforms with very little out-of-band energy but, again, does not restrict the power that can be transmitted inside the ISM band.)

The system must of course still respect safety limits. For near-field systems such as FREE-D, compliance with safety regulations must be evaluated in terms of specific absorption rate (SAR), measured in W/kg, and the associated basic restrictions. The use of incident field strength (measured in V/m [electric field] or A/m [magnetic field]) and the associated reference levels significantly overestimate human exposure. In a prior study, the authors collaborated with Dr Niels Kuster of The Foundation for Research on Information Technologies in Society and Eidgenössische Technische Hochschule: The Swiss Federal Institute of Technology, Zurich to numerically calculate SAR in humans for several representative wireless power transmitter configurations. **Fig. 9** shows three representative transmit resonator configurations studied; **Fig. 10** shows calculated SAR. SAR was calculated for four detailed anatomic human models, known as the "virtual family." For the resonator and body geometries studied, 45 W was the lowest transmit power level at which a basic restriction was reached, which is higher than the power level the authors are proposing to use.

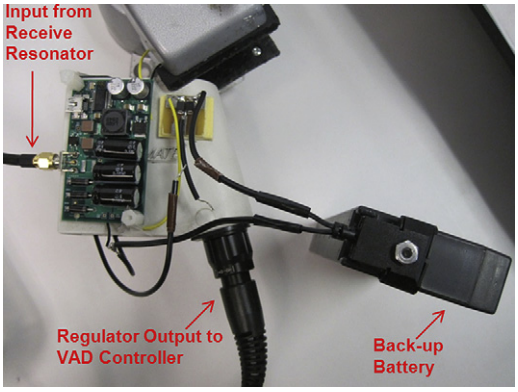

Fig. 7. RF-DC rectifier and DC-DC regulator circuit with back-up battery.

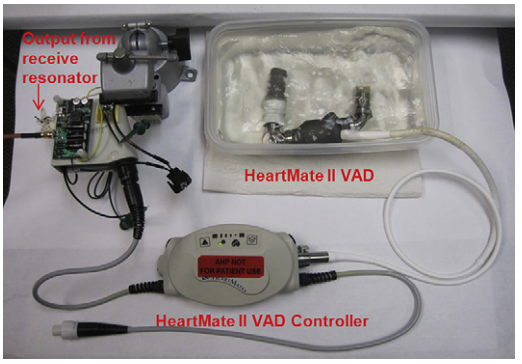

Fig. 8. RF-DC rectifier and DC-DC converter circuit in line with HeartMate II VAD and VAD controller.

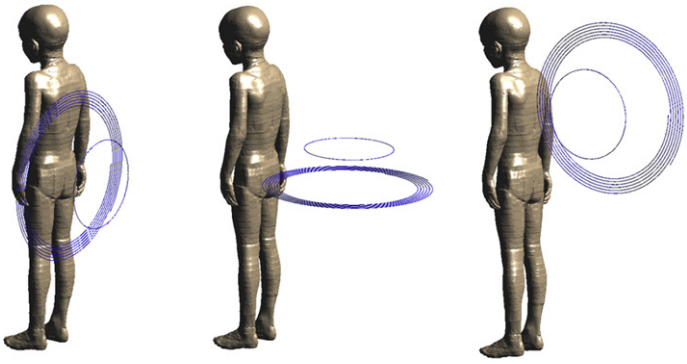

Fig. 9. Three representative resonator configurations studied: coronal, axial, sagittal.

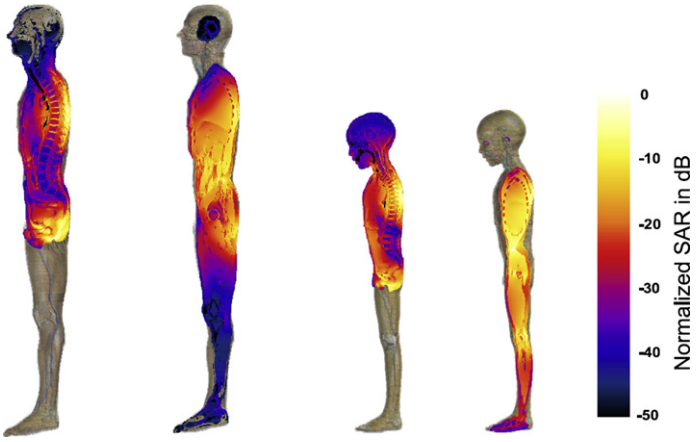

Fig. 10. Local SAR in the models Duke and Thelonius in two sagittal planes (centered and 75 mm off-center) for coronal exposure.

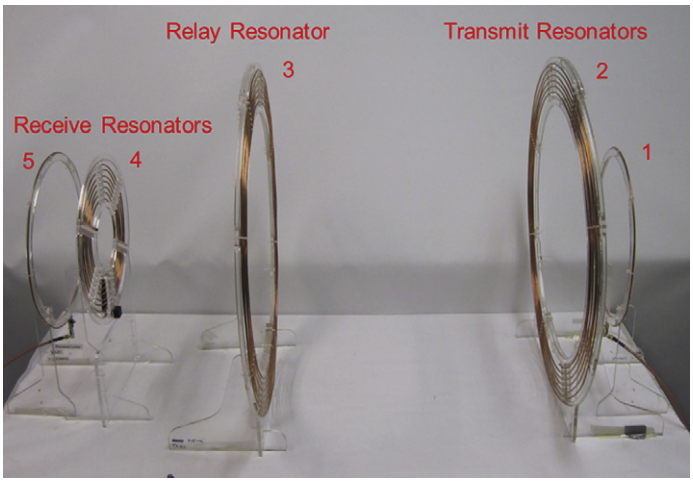

Fig. 11. Experiment 1 resonator configuration.

Table 2
Experiment 1 resonator dimensions and separation distances

	Resonator 1	Resonator 2	Resonator 3	Resonator 4	Resonator 5
Outer diameter (cm)	31.0	59.0	59.0	28.0	31.0
Distance from 1 (cm)	0.00	6.35	59.7	90.2	100

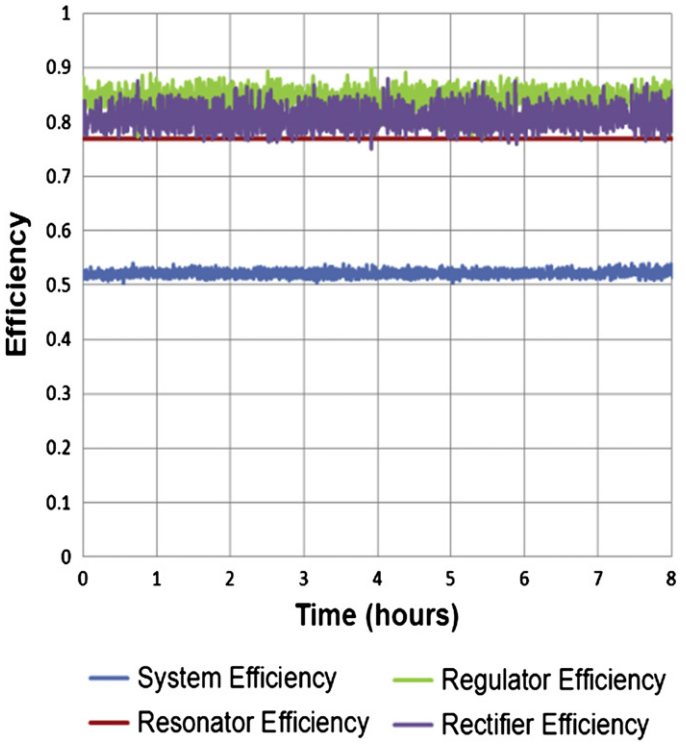

Fig. 12. Experiment 1 efficiency characteristic.

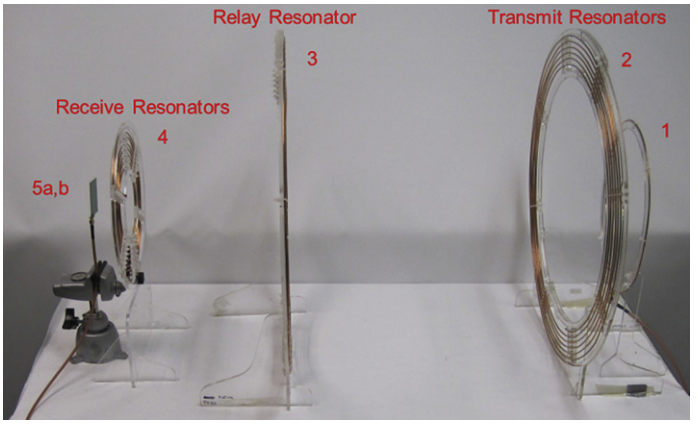

Fig. 13. Experiment 2 resonator configuration.

Table 3
Experiment 2 resonator dimensions and separation distances

	Resonator 1	Resonator 2	Resonator 3	Resonator 4	Resonator 5a	Resonator 5b
Outer diameter (cm)	31.0	59.0	59.0	28.0	5.70	4.30
Distance from 1 (cm)	0.00	6.35	59.7	90.2	99.8	100

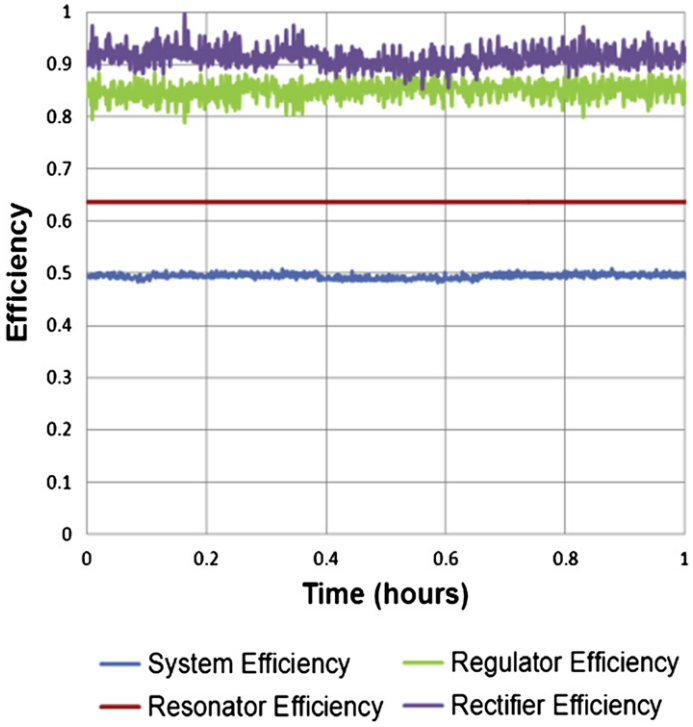

Fig. 14. Experiment 2 efficiency characteristic.

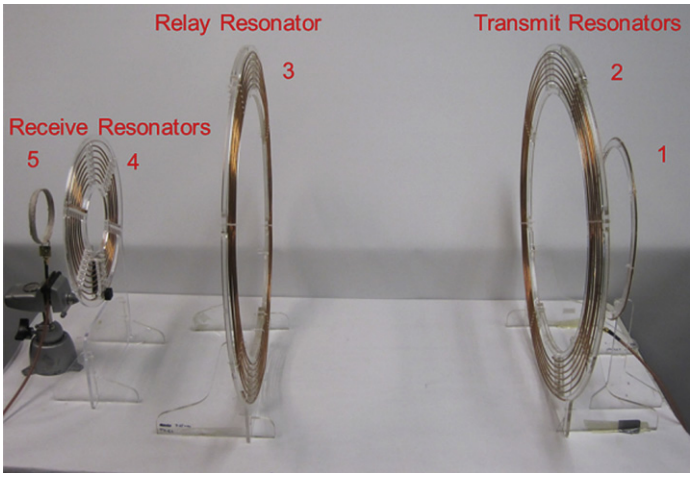

Fig. 15. Experiment 3 resonator configuration.

Table 4
Experiment 3 resonator dimensions and separation distances

	Resonator 1	Resonator 2	Resonator 3	Resonator 4	Resonator 5
Outer diameter (cm)	31.0	59.0	59.0	28.0	9.50
Distance from 1 (cm)	0.00	6.35	59.7	90.2	100

FREE-D EXPERIMENTAL ANALYSIS

The system in **Fig. 6** was experimentally tested using the FREE-D wireless power system and the HeartMate II (Thoratec Corporation) and VentrAssist VADs (VentraCor, Ltd, Chatswood, Australia). Six separate experiments were conducted to monitor the following FREE-D system properties:

1. Power delivery with a static, 1-m separation distance between transmit and receive resonators using both the HeartMate II and VentrAssist VADs.
2. Power delivery throughout an extended duration of FREE-D operation.
3. Temperature of the receive resonator.
4. Power delivery via relay resonators for various receive resonator sizes.
5. Power delivery with a static FREE-D configuration for all VentrAssist VAD pump speeds.

Experiment 1

The configuration for experiment 1 (**Fig. 11**) operated continuously for 8 hours without any loss of power delivered to the left ventricular assist device. The resonator sizes and distances between each resonator can be seen in **Table 2**. The large, copper receive resonator temperature started at 71°F, rose steadily over the course of approximately 1 hour to 82°F, and remained constant for the next 7 hours. The efficiencies (power out divided by power in) for the transmit-receive resonators, RF-DC rectifier, DC-DC regulator, and system efficiency are shown in **Fig. 12**. The data for these efficiency

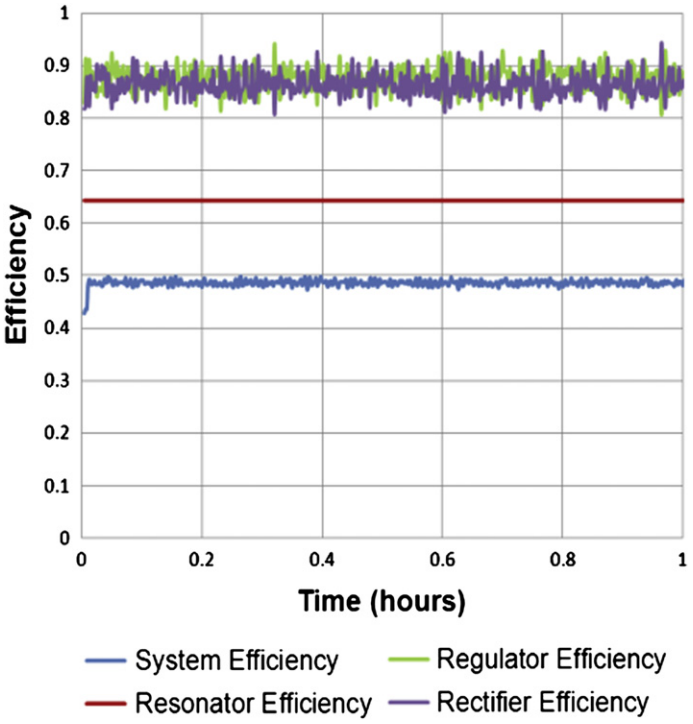

Fig. 16. Experiment 3 efficiency characteristic.

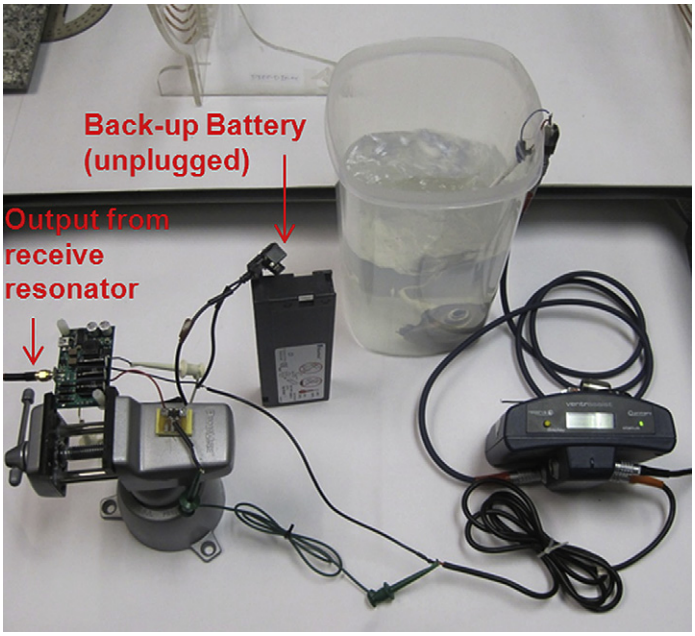

Fig. 17. RF-DC rectifier and DC-DC converter circuit in line with MagLev VAD and VAD (Ventracor, Chatswood, Australia) controller.

Table 5
Experiment 6 resonator dimensions and separation distances

	Resonator 1	Resonator 2	Resonator 3	Resonator 4	Resonator 5
Outer diameter (cm)	31.0	59.0	59.0	28.0	9.50
Distance from 1 (cm)	0.00	12.5	60.7	83.6	90.0

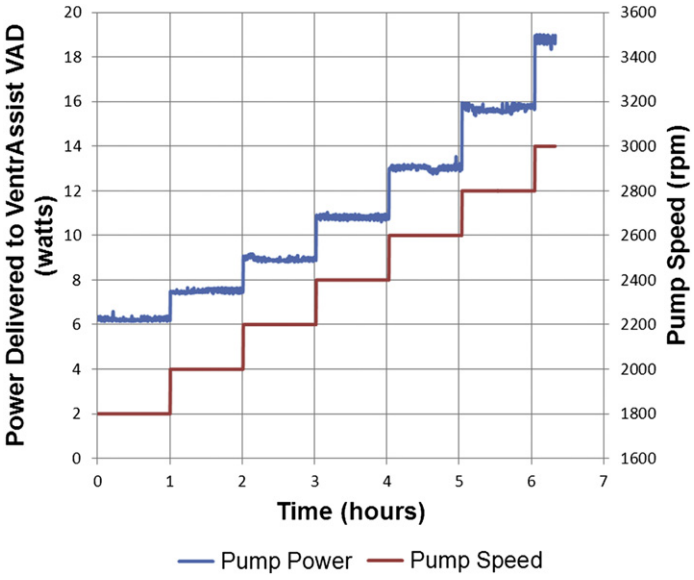

Fig. 18. Pump power and pump speed over 7 hours continuous functioning of a Ventrassist pump, with an uninterrupted power supply by the FREE-D system.

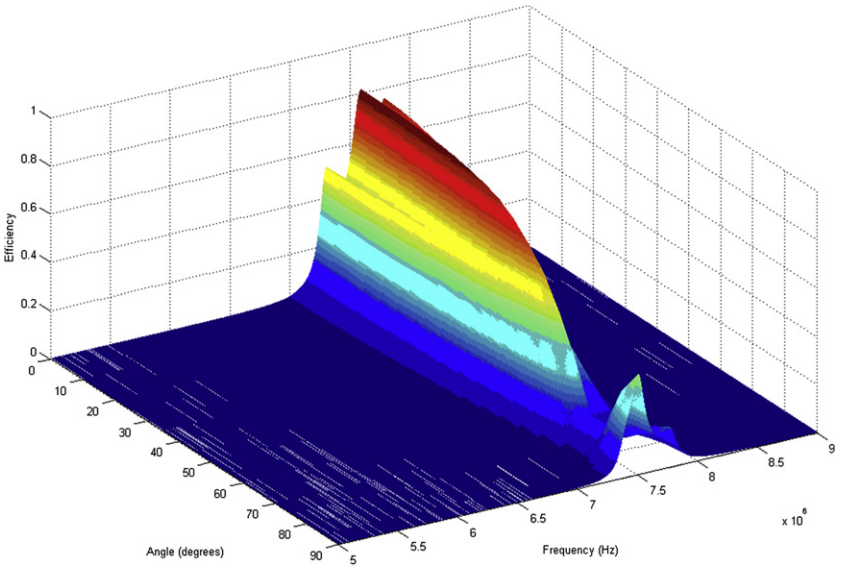

Fig. 19. Plot for FREE-D resonator efficiency as a function of resonator angular misalignment and frequency.

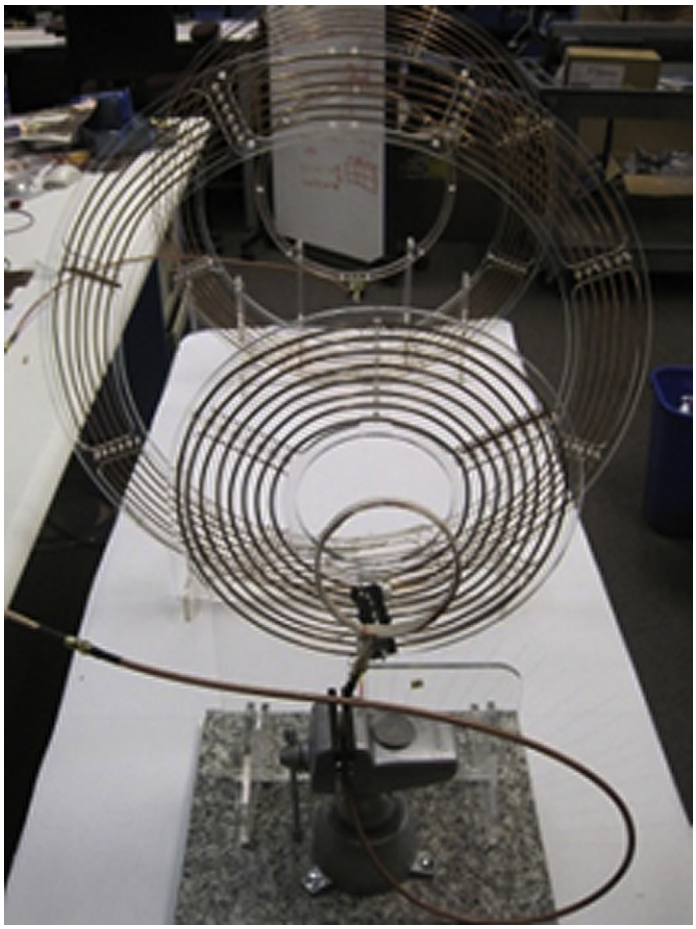

Fig. 20. The effects that an angular misalignment between the transmit and receive resonators have on system efficiency (receive coil facing the transmitting coil).

calculations were logged continuously over the entire 8-hour duration, and the constant efficiency curves verify the successful operation of this experiment.

Experiment 2

The configuration for experiment 2 (**Fig. 13**) operated continuously for 1 hour while using a small, printed circuit board (PCB) receive resonator. The resonator sizes and distances between each resonator can be seen in **Table 3**. The receive PCB resonator temperature rapidly rose to 153°F in 7 minutes, and then remained steady at 146°F for the duration of the experiment. This temperature rise is caused by the properties of the PCB material, and is addressed in experiment 3 using a non-PCB resonator. **Fig. 14** shows the efficiencies for each component in the FREE-D system for this experiment.

Experiment 3

The configuration for experiment 3 (**Fig. 15**) operated continuously for 1 hour. The resonator sizes and distances between each resonator can be seen in **Table 4**. The small, copper receive resonator temperature rose from an initial temperature of 77°F to 87°F in 7 minutes, and then remained constant at 86°F for the duration of the experiment. **Fig. 16** shows the efficiencies for each component in the FREE-D system.

For each experiment, the average rectifier and regulator efficiencies remain nearly the same. Therefore, the system efficiency is primarily controlled by the transmit–receive resonator efficiency, which changes according to the size of the receive resonators used in each experiment. With the large receive resonator in experiment 1, the resonator efficiency is highest, whereas the small PCB resonator has the worst efficiency. Therefore, the smaller the receive resonator, the more sensitive the power efficiency will be to misalignments between the relay resonator

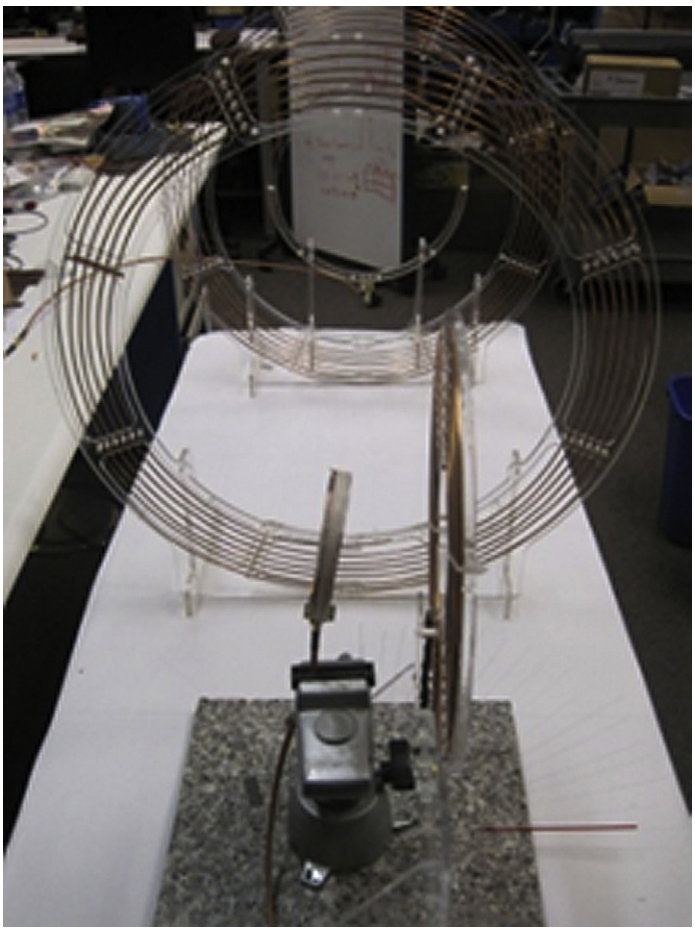

Fig. 21. The effects that an angular misalignment between the transmit and receive resonators have on system efficiency (receive coil at right angles to the transmitting coil).

embedded in a vest and the receive resonator implanted in the body.

Experiment 4

The configuration for experiment 4 (**Fig. 17**) operated continuously for 2 weeks over a full range of pump speeds for the VentrAssist Magnetic Levitation VAD (Ventracor, Ltd). The resonators used were identical to those in experiment 3 (see **Fig. 15**); however, the separation distances were modified slightly, as can be seen in **Table 5**. These modified separation distances allow for a resonator efficiency of 90% or greater. Data were logged using the VentrAssist VentraView VV10_0 software. Also, the VAD pump speed was varied from 1800 to 3000 revolutions per minute (rpm) by increments of 200 rpm. As the pump speed increases, the power demanded by the pump also increases. Therefore, the input power to the transmit resonator was increased manually each time the pump speed was increased to meet the power needs of the VAD. **Fig. 18** shows the efficiencies for each component in the FREE-D system over the full 2-week duration of the experiment for the varying pump speeds.

Experiment 5

The configuration for experiment 5 (same as experiment 3 as shown in **Fig. 15**) shows the effects that an angular misalignment between the transmit and receive resonators have on system efficiency. **Fig. 19** shows the relationship between efficiency and angular misalignment, and **Figs. 20** and **21** show the experimental configuration.

Experiment 6

Experiment 6 shows how efficiency and frequency tuning are affected when ham (which is similar in electrical conductivity to the human body) comes in close proximity to the receive resonator. Each slab of ham is 17.33-mm thick, with an approximated capacitance of C_{HAM} = picofarads Two different materials and sizes of resonators were tested in this experiment, as outlined in **Table 6** and shown in **Figs. 22** and **23**.

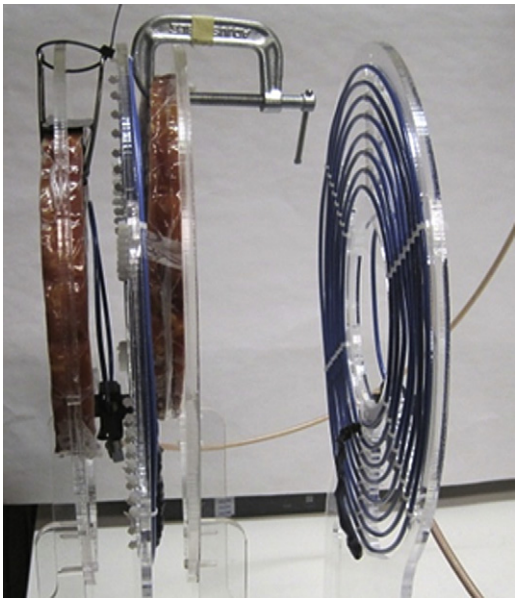

Fig. 22. Insulated copper resonators with ham in physical contact with the receive resonator.

Several different configurations were tested to determine whether the presence of ham will have a negative effect on resonator efficiency: no ham present, ham nearby resonators, ham in physical contact with the resonators, and metal nearby the resonators. **Figs. 24** and **25** compare the effects on efficiency for each of these configurations for both resonators tested.

The ham's ability to detune the receive resonator has a more harmful effect on the efficiency of the wireless power transfer than its potential to act as a flux interceptor. However, regardless of the reason, the quality factor of the resonators is reduced for all configurations. Coil design becomes very important when considering how

Table 6
Experiment 6 resonator characteristics

	Resonator Diameter (cm)	Resonator Capacitance (pF)
Insulated (blue) copper resonators	28.0	25.0
PCB resonators	4.30	1000

Fig. 23. PCB resonators with ham in physical contact with the receive resonator.

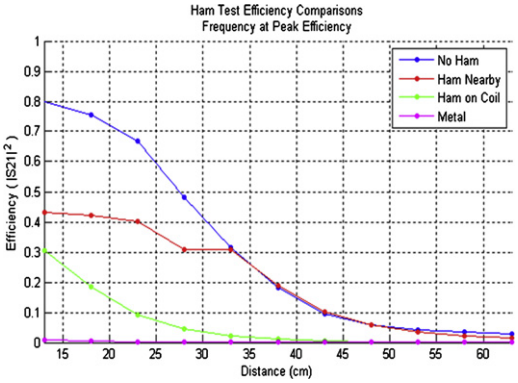

Fig. 24. Experiment 6 efficiency insulated (*blue*) copper resonator efficiency analysis.

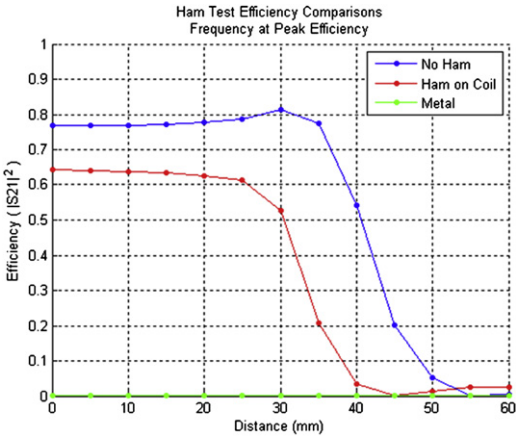

Fig. 25. Experiment 6 efficiency PCB resonator efficiency analysis.

to minimize the detuning effect when ham or human body tissue comes within close range of the receive resonator. Increasing the inductance of a resonator is desirable to maximize the quality factor Q of a coil. However, if the inductance is so large that the required trimming capacitance of the resonator for the desired resonant frequency $\left(f = 1/2\pi\sqrt{LC}\right)$ is on the same order of magnitude as the capacitance of the ham, the efficiency of the system will be worse. Research must be performed on the capacitance of the tissues in the human body where the resonators are likely to be implanted to determine a minimum threshold for trimming capacitance and an ideal balance between *L* and *C* of the resonators when considering optimal resonator designs. Impedance matching techniques may solve the reduced efficiency with ham present for the PCB resonators.

SUMMARY

The authors' vision constitutes a completely implantable cardiac assist system affording tether-free mobility in an unrestricted space powered wirelessly by the innovative FREE-D system (**Fig. 26**). Patients will have no power drivelines traversing the skin, and this system will allow power to be delivered over room distances and will eliminate trouble-prone wirings, bulky consoles, and replaceable batteries.

The authors envisage converting living spaces to a safe all-encompassing environment in which patients are able to receive power no matter whether they are in their home, office, or car. This system is

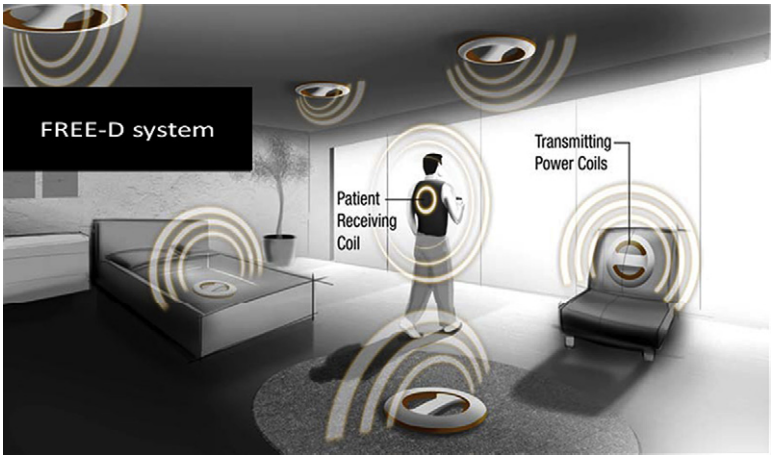

Fig. 26. FREE-D system.

unlike any older TET system, which had the disadvantages of reliability, contact burns, or irritation. The advantages of the FREE-D system range from reduced potential for life-threatening infections, better patient safety, and improved quality of life.

REFERENCES

1. Deng MC, Edwards LB, Hertz MI, et al. Mechanical circulatory support device database of the International Society for Heart and Lung Transplantation: first annual report–2003. J Heart Lung Transplant 2003;22(6):653–62.
2. Holman WL, Kormos RL, Naftel DC, et al. Predictors of death and transplant in patients with a mechanical circulatory support device: a multi-institutional study. J Heart Lung Transplant 2009;28(1):44–50.
3. Miller LW, Pagani FD, Russell SD, et al. HeartMate II Clinical Investigators. Use of a continuous-flow device in patients awaiting heart transplantation. N Engl J Med 2007;357(9):885–96.
4. Pagani FD, Miller LW, Russell SD, et al. HeartMate II Investigators. Extended mechanical circulatory support with a continuous-flow rotary left ventricular assist device. J Am Coll Cardiol 2009;54(4):312–21.
5. Slaughter MS, Rogers JG, Milano CA, et al. HeartMate II Investigators. Advanced heart failure treated with continuous-flow left ventricular assist device. N Engl J Med 2009;361(23):2241–51.
6. Genovese EA, Dew MA, Teuteberg JJ, et al. Incidence and patterns of adverse event onset during the first 60 days after ventricular assist device implantation. Ann Thorac Surg 2009; 88(4):1162–70.
7. Martin SI, Wellington L, Stevenson KB, et al. Effect of body mass index and device type on infection in left ventricular assist device support beyond 30 days. Interact Cardiovasc Thorac Surg 2010;11(1): 20–3.
8. Holman WL, Pamboukian SV, McGiffin DC, et al. Device related infections: are we making progress? J Card Surg 2010;25(4):478–83.
9. Raymond AL, Kfoury AG, Bishop CJ, et al. Obesity and left ventricular assist device driveline exit site infection. ASAIO J 2010;56(1):57–60.
10. Zierer A, Melby SJ, Voeller RK, et al. Late-onset driveline infections: the Achilles' heel of prolonged left ventricular assist device support. Ann Thorac Surg 2007;84(2):515–20.
11. Allen JG, Weiss ES, Schaffer JM, et al. Quality of life and functional status in patients surviving 12 months after left ventricular assist device implantation. J Heart Lung Transplant 2010;29(3):278–85.
12. Wilson W, Taubert KA, Gewitz M, et al. Prevention of infective endocarditis. J Am Dent Assoc 2008; 139(Suppl):3S–24S.
13. Baddour LM, Bettmann MA, Bolger AF, et al. Nonvalvular cardiovascular device-related infections. Circulation 2003;108(16):2015–31.
14. Kurtz SM, Lau E, Schmier J, et al. Infection burden for hip and knee arthroplasty in the United States. J Arthroplasty 2008;23(7):984–91.
15. Holman WL, Park SJ, Long JW, et al. REMATCH Investigators. Infection in permanent circulatory support: experience from the REMATCH trial. J Heart Lung Transplant 2004;23(12):1359–65.
16. Gordon RJ, Quagliarello B, Lowy FD. Ventricular assist device-related infections. Lancet Infect Dis 2006;6(7):426–37.
17. Monkowski DH, Axelrod P, Fekete T, et al. Infections associated with ventricular assist devices: epidemiology and effect on prognosis after transplantation. Transpl Infect Dis 2007;9(2):114–20.
18. Baddour LM, Epstein AE, Erickson CC, et al. Update on cardiovascular implantable electronic device infections and their management: a scientific statement from the American Heart Association. Circulation 2010;121(3):458–77.
19. Schaffer JM, Allen JG, Weiss ES, et al. Infectious complications after pulsatile-flow and continuous-flow left ventricular assist device implantation. J Heart Lung Transplant 2011;30(2):164–74.
20. Topkara VK, Kondareddy S, Malik F, et al. Infectious complications in patients with left ventricular assist device: etiology and outcomes in the continuous-flow era. Ann Thorac Surg 2010;90(4):1270–7.
21. Siegenthaler MP, Martin J, Pernice K, et al. The Jarvik 2000 is associated with less infections than the HeartMate left ventricular assist device. Eur J Cardiothorac Surg 2003;23(5):748–54 [discussion: 754–5].
22. Holman WL, Kirklin JK, Naftel DC, et al. Infection after implantation of pulsatile mechanical circulatory support devices. J Thorac Cardiovasc Surg 2010; 139(6):1632, e2–6.
23. Dew MA, Kormos RL, Winowich S, et al. Human factors issues in ventricular assist device recipients and their family caregivers. ASAIO J 2000;46(3): 367–73.
24. Kormos RL, Teuteberg JJ, Pagani FD, et al. HeartMate II Clinical Investigators. Right ventricular failure in patients with the HeartMate II continuous-flow left ventricular assist device: incidence, risk factors, and effect on outcomes. J Thorac Cardiovasc Surg 2010;139(5):1316–24.
25. Hravnak M, George E, Kormos RL. Management of chronic left ventricular assist device percutaneous lead insertion sites. J Heart Lung Transplant 1993; 12(5):856–63.
26. Haj-Yahia S, Birks EJ, Rogers P, et al. Midterm experience with the Jarvik 2000 axial flow left ventricular assist device. J Thorac Cardiovasc Surg 2007; 134(1):199–203.

27. El-Banayosy A, Arusoglu L, Kizner L, et al. Preliminary experience with the LionHeart left ventricular assist device in patients with end-stage heart failure. Ann Thorac Surg 2003;75(5):1469–75.
28. Bonde P, Bermudez C, Lockard KL, et al. The Ventricular Assist Device (VAD) Driveline: What is The Price of Living with This Technology? International Society of Heart Lung Transplantation. 30th Annual Meeting and Scientific Sessions. Chicago, 2010.
29. Bonde P, Dew MA, Meyer D, et al. National Trends in Readmission (REA) Rates Following Left Ventricular Assist Device (LVAD) Therapy, International Society of Heart Lung Transplantation. 31st Annual Meeting. San Diego, April 15, 2011.